



Contents lists available at ScienceDirect

# Journal of Science and Medicine in Sport

journal homepage: [www.elsevier.com/locate/jsams](http://www.elsevier.com/locate/jsams)



Original research

## Proposed injury thresholds for concussion in equestrian sports

J. Michio Clark<sup>a</sup>, Kevin Adanty<sup>b</sup>, Andrew Post<sup>c,b,a</sup>, T. Blaine Hoshizaki<sup>b</sup>,  
Jonathan Clissold<sup>d</sup>, Adrian McGoldrick<sup>e</sup>, Jerry Hill<sup>f</sup>, Aisling Ni Annaidh<sup>a</sup>,  
Michael D. Gilchrist<sup>a,b,\*</sup>

<sup>a</sup> School of Mechanical & Materials Engineering, University College Dublin Belfield, Ireland

<sup>b</sup> Faculty of Health Sciences, School of Human Kinetics, University of Ottawa, Canada

<sup>c</sup> St. Michael's Hospital, Canada

<sup>d</sup> British Eventing, United Kingdom

<sup>e</sup> Irish Horseracing Regulatory Board, Ireland

<sup>f</sup> British Horseracing Authority, United Kingdom

### ARTICLE INFO

#### Article history:

Received 2 June 2019

Received in revised form

12 September 2019

Accepted 7 October 2019

Available online xxx

#### Keywords:

Head impact biomechanics

Brain injury

Accident reconstruction

Equestrian helmet

### ABSTRACT

**Objectives:** Equestrian helmets are designed to pass certification standards based on linear drop tests onto rigid steel surfaces. However, concussions in equestrian sports occur most commonly when a rider is thrown off a horse and obliquely impacts a compliant surface such as turf or sand. This paper seeks to elucidate the mechanics of such impacts and thereby propose corresponding thresholds for the occurrence of concussion that can improve equestrian helmet standards and designs.

**Design:** The present study examined the biomechanics of real-world equestrian accidents and developed thresholds for the occurrence of concussive injury.

**Methods:** Twenty-five concussive and 25 non-concussive falls in equestrian sports were reconstructed using a combination of video analysis, computational and physical reconstruction methods. These represented male and female accidents from horse racing and the cross-country phase of eventing.

**Results:** The resulting thresholds for concussion [59 g, 2700 rad/s<sup>2</sup>, 28 rad/s, 0.24 (MPS), 6.6 kPa and 0.27 (CSMD<sub>10</sub>) for 50% risk] were consistent with those reported in the literature and represent a unique combination of head kinematic thresholds compared to other sports. Current equestrian helmet standards commonly use a threshold of 250 g and a linear drop to a steel anvil resulting in less than 15 ms impacts. This investigation found that concussive equestrian accidents occurred from oblique impacts to turf or sand with lower magnitude and longer duration impacts (<130 g and >20 ms). This suggests that current equestrian helmet standards may not adequately represent real-world concussive impact conditions and, consequently, there is an urgent need to assess the protective capacity of equestrian helmets under real-world conditions.

© 2019 Sports Medicine Australia. Published by Elsevier Ltd. This is an open access article under the CC BY-NC-ND license (<http://creativecommons.org/licenses/by-nc-nd/4.0/>).

### 1. Introduction

Over the past decade there has been increasing attention given to the need to prevent concussion. The increased awareness of the growing epidemic of concussion has largely been due to research that identified how multiple concussions over the period of an athlete's career could lead to long term disability.<sup>1–3</sup> In equestrian sports, the use of helmets has reduced the occurrence of TBIs.<sup>4–6</sup> However, concussions remain among the most common injuries sustained from accidents across all equestrian sports.<sup>7,8</sup> As a result,

more research is required to understand the impact mechanics of concussive events in equestrian sports to improve injury prevention efforts through helmet design.

Currently, equestrian helmets are designed to pass certification standards that involve a linear drop test onto a rigid steel surface.<sup>9–11</sup> In equestrian sports there is a risk of impacting rigid surfaces such as a horse's hoof, concrete ground or a fence, however, there is a higher probability of the rider's head impacting softer surfaces such as turf and sand.<sup>12</sup> Concussions in equestrian sports are most commonly a result of being thrown off the horse and impacting these soft surfaces. This results in an oblique impact to a compliant surface, the mechanics of which have not been widely studied. Understanding the event characteristics and mechanics

\* Corresponding author.

E-mail address: [michael.gilchrist@ucd.ie](mailto:michael.gilchrist@ucd.ie) (M.D. Gilchrist).

<https://doi.org/10.1016/j.jsams.2019.10.006>

1440-2440/© 2019 Sports Medicine Australia. Published by Elsevier Ltd. This is an open access article under the CC BY-NC-ND license (<http://creativecommons.org/licenses/by-nc-nd/4.0/>).

which lead to concussions in equestrian sports will have significant implications for equestrian helmet standards and helmet designs.

Most of the literature relating to the reconstruction of real-world concussions is from studies involving research in American football, rugby, and Australian rules football.<sup>13,14</sup> That research has been used to determine the risk of sustaining a concussion based on head kinematics and brain tissue response measurements.<sup>15–17</sup> However, those sports represent different impact kinematics when compared to equestrian sports and, as a result, the associated concussion injury thresholds may not translate to equestrian sports. Unique impact parameters such as location, mass, velocity, direction and compliance have been shown to influence head kinematic and brain tissue response.<sup>18</sup> These unique impact parameters can also influence the protective capacity of helmets and must be understood in order to optimise head protection in their respective sports. As a result, little is known about the impact mechanics that lead to concussion in equestrian sports and how helmets perform under these conditions.

Some preliminary accident investigations have been conducted in equestrian sports.<sup>12,19,20</sup> However, due to small sample sizes and the use of representative rather than real-world reconstructions to determine impact parameters, limited conclusions can be drawn from those studies. Further research is needed to better understand the real-world loading conditions associated with concussions in equestrian sports. The purpose of this study was to examine the biomechanics of real-world equestrian accidents and develop associated thresholds for the occurrence of concussive injury.

## 2. Methods

A total of 1119 accidents in which riders fell off their horses in either racing or the cross-country phase of eventing were collected from governing bodies in Ireland and Britain. The video and corresponding accident data was collected between August 2011 and May 2018. In this study, both concussive and non-concussive cases were analysed. Concussive head impacts were defined as a rider who had received an impact to the head and was diagnosed by a medical doctor as having a concussion. Non-concussive incidents were identified as those in which a head impact occurred, but no head injury was reported during or after the event. The inclusion/exclusion criteria for concussive and non-concussive cases were as follows:

- 1 Have a clear view of the impact.
- 2 Be able to produce a reliable calibration (see Supplementary Material)
  - a. at least one camera angle between 0° and 60°
  - b. calibration is parallel to the line of action
- 3 The incident must be a fall event where the rider's head hits the ground
- 4 Incidents with multiple head impact events were excluded (e.g. fall and kicked)

Of the initial 1119 videoed equestrian accidents, 114 were of concussive cases and 25 cases met the inclusion criteria. An equal number of non-concussive cases were then selected for reconstruction. In addition to the inclusion criteria above, the non-concussive cases were also selected to match the impact location and direction of the concussive cases as closely as possible. This selection criteria was regarded as important instead of selecting random non-concussive cases, as it has been well-documented that impact direction influences the risk of injury. By matching impact location and direction as closely as possible, it was intended to remove any directional bias between the two groups and be able to evaluate the risk of concussion using as closely matched pairs as possible.

All other variables (e.g. fall height/impact velocity, trajectory angle, Going Rating/compliance) were not controlled and differences in these variables would be a consequence of the fundamental differences between concussive and non-concussive groups. When multiple non-concussive cases matched a concussive case, the non-concussive case that was reconstructed was selected randomly.

Both concussive and non-concussive falls in equestrian sports were reconstructed using a combination of video analysis, computational and physical reconstruction methods. Video analysis was conducted using Kinovea 0.8.20 (open source, kinovea.org.) to identify the type of event (e.g. fall, kick or collision), the head impact location, the impact surface (e.g. turf, sand, horse hoof or horse leg), as well as the horizontal velocity, height of the rider's head and jockey/rider's body position prior to impact. This software has been used previously<sup>21</sup> in the field of brain injury biomechanics to define impact parameters such as velocity, orientation and location for laboratory experiments, computational simulations, and coupled with on-field measurements using the Head Impact Telemetry (HIT) System. Mathematical Dynamic Models (MADYMO) version 7.6 simulations were conducted based on body position, impact location and velocity as determined from video analysis. This software has been widely used to reconstruct the kinematics of the human body for falling scenarios.<sup>20,22</sup> These simulations were performed in order to determine impact velocity and trajectory angle at contact. Experimental reconstructions were conducted using a helmeted Hybrid III headform and rail guided launcher (RGL) according to the impact parameters (location, compliance, velocity, angle) determined from the video and MADYMO analysis. Experimental reconstructions were performed to provide comparable data for separate physical helmet tests. Accident report forms were used to confirm the Going Rating on the day of the accident and one of three representative anvils was used to reflect the compliance of the surface for the reconstructions.<sup>23</sup> Three impacts were conducted for each case and the resulting head kinematics (linear acceleration, rotational velocity and rotational acceleration) were measured directly from the accelerometers and angular rate sensors in the Hybrid III headform. Linear and rotational acceleration-time histories obtained from the headform were used subsequently as loading conditions in the UCDBTM<sup>24,25</sup> which was then used to calculate maximum principal strain (MPS) von Mises stress (VMS) and the 10% cumulative strain damage measure (CSDM<sub>10</sub>) in the cerebrum.

Impact location was determined using a reference shown in Fig. 1. Using this reference, the head was divided into 30 sections. In the transverse plane the head was divided into 8 sections and in the sagittal plane 5 levels were created. The transverse sections were segmented into equal 45° segments. For the sagittal sections, the head was segmented by creating horizontal sections every 6 cm with respect to the 50th Hybrid III headform, starting from the chin and proceeding superiorly. This created four evenly spaced levels plus a smaller 2.5 cm top (crown) level in the sagittal plane. The precision level of Fig. 1 to identify impact location in this study was similar to other studies reporting impact location.<sup>13,26</sup>

In order to determine horizontal velocity and height of the rider's head prior to falling from the horse, it was necessary to establish a scaling reference. This was created from known 50th percentile male and 5th percentile female anthropometrics (e.g. sitting height, leg length) or known distances on the racetrack (e.g. distance between fence posts, height of jumps or fence posts). By establishing an accurate reference scale, a linear calibration can be determined allowing pixels to be converted to meters (Figs. 2 and 3). This allowed for distances and heights on the racetrack/cross country course to be quantified. The horizontal velocity was subsequently calculated by measuring the distance a rider had travelled between a given number of video frames. The distance measurement was along the principle line of action (i.e. resultant)

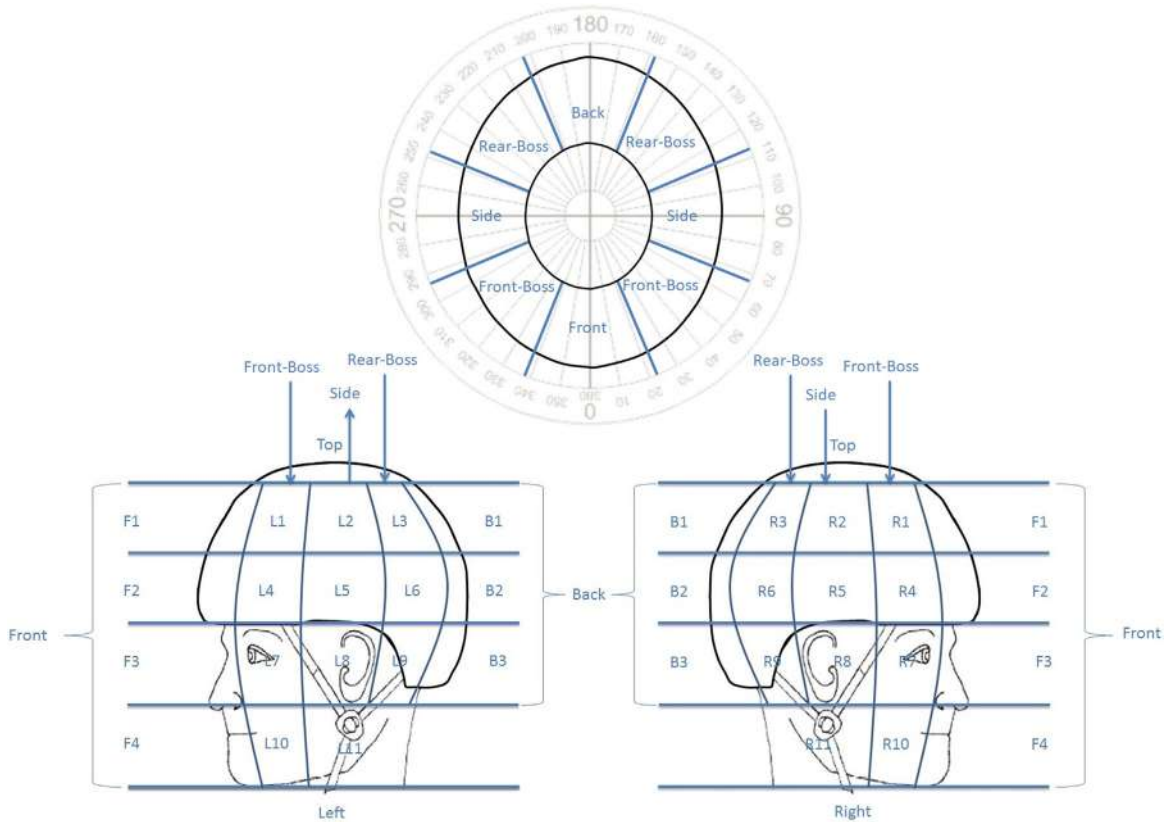


Fig. 1. Left and Right view of the helmeted head illustrating divisions used to identify impact location for accident reconstruction.



Fig. 2. Example of velocity measurement using a line calibration in horse racing. The green line represents the distance from the top of the jockey's head to their right knee and the red line represents the distance the jockey's head travelled after the jump to impact. (For interpretation of the references to color in this figure legend, the reader is referred to the web version of this article.)

with respect to the ground ( $x-y$  plane). Videos were recorded at known frame rates of between 23.97 and 30 fps depending on the video source. As with all measurements there are associated errors. An evaluation of the measurement uncertainty of this video anal-

ysis method is presented in the Supplementary Material. In short, the results showed that the uncertainty associated with the measurement of horizontal and vertical distance was no more than 25% and 11%, respectively using the method described above. The



**Fig. 3.** Example of measurement for jockey head height using a line calibration in horse racing where the height of the fence is known and is taken as the vertical reference height.

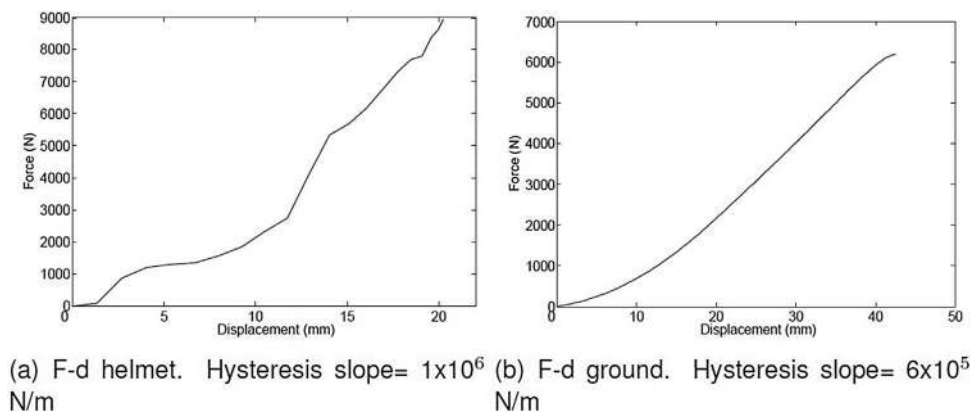


**Fig. 4.** Force-displacement curves for helmet (a) and ground (b).<sup>19</sup> Linear hysteresis models were used to the unloading portion.

uncertainty associated with the horizontal and vertical distance measurements are similar to the uncertainty in quantifying impact velocity when using Kinovea and similar methods (5–22%).<sup>21</sup>

The MADYMO reconstructions were conducted with either the 5th percentile female pedestrian model to represent female riders, or 50th percentile male ellipsoid pedestrian model to represent male riders. As all riders wore a helmet, all models were modified to include a helmet. The helmet was created using a single ellipsoid with helmet geometry and properties obtained from a baseline equestrian helmet. The helmet was attached to the pedestrian model using a bracket joint (a rigid joint between two bodies). The stiffness of the ground was also modified to represent the loading force–displacement characteristics of turf.<sup>19</sup> Fig. 4 presents the loading force–displacement characteristics for the helmet and ground.<sup>19</sup> Linear hysteresis models were used to the unloading portion. A friction coefficient of 0.5 was assumed for contact between the helmet and the ground.

The appropriate female or male ellipsoid model was placed within the simulation environment and simulations were conducted based on body position, impact location and velocity as determined from video analysis. The starting point for all simu-

lations was when the rider was ejected from the saddle and the motion of the rider could be considered passive. This starting point was chosen so it was possible to model the accident using a passive pedestrian model. As all simulations were started when the jockey had already been unseated from the horse, initial downward and horizontal velocities were applied to the model. An initial horizontal velocity was applied to the model which was determined from video analysis and the downward velocity was determined by using video analysis in conjunction with the height of the rider’s head in the MADYMO simulation. The initial downward velocity applied to the model was selected to ensure the time to impact was the same in the video as the simulation. All simulations were assessed visually to ensure the body kinematics of the model were as close an approximation as possible to the jockey/rider in the video (Fig. 5). A series of MADYMO simulations were conducted for each case by varying horizontal and vertical velocity by  $\pm 10\%$  according to the error in measurement (see Supplementary Material), and other similar video analysis methods.<sup>21</sup> The head impact velocities at contact determined in the MADYMO reconstructions along with the corresponding trajectory angle were obtained. The slowest impact velocity and associated trajectory angle at contact





**Fig. 5.** An example of frame by frame snap shots (left) to assess approximation of the model's body kinematics of a jockey (right) during an accident in horse racing.

were obtained from a series of MADYMO simulations for each case. The slowest impact velocity and associated trajectory angle at contact were selected for each case as the designated “best possible scenario” for the simulations.

Hybrid III headforms were used as human head surrogates. Both the 5th percentile female and the 50th percentile male Hybrid III headforms (3.73 ± 0.01 kg and 4.54 ± 0.01 kg, respectively) were used. The headforms were equipped with Diversified Technical Systems (DTS) 6DX PRO attached to a SLICE NANO data acquisition system. The DTS 6DX PRO has three linear accelerometers and three angular rate sensors to measure linear acceleration and rotational velocity. Signals from the accelerometers and angular rate sensors were collected at 20 kHz and filtered with a 300 Hz low pass Butterworth filter in accordance with the SAE J211 convention (SAE

2007). Signals were filtered at 300 Hz to minimize the noise generated by differentiating data obtained from angular rate sensors. In order to estimate rotational acceleration, the measured rotational velocity time-histories were differentiated.

The headforms were fitted with a commercially available jockey helmet. The helmets had a circumference of 54 cm for the 5th percentile female and 59 cm for the 50th percentile male. The shell of the helmet was made of fiberglass and was 2 mm thick. The helmet liners consisted of 18–20 mm 64 g/l expanded polystyrene. The helmets also included an internal foam block at the crown of the helmet which was 50 × 50 mm and 10–15 mm thick. The foam block at the crown of the helmet created an air gap between the shell and the liner.

The rail guided launcher (RGL) was used for all conducted experimental reconstructions in this study (Fig. 6). The launcher consisted of two 3.3 m long rails attached to a frame. At one end of the frame sat an electric motor which powered two trailer wheels used to accelerate the carriage down the rails. The headform was attached to the carriage and the carriage ran along the rails on ball bearing bushings to reduce the influence of friction on the inbound velocity of the headform. At the other end of the frame was a foam stopper which allowed the headform to be launched from the carriage as the carriage was stopped and the headform continued on its trajectory. The frame to which the rails were attached was adjustable between 0° and 30° with increments every 5°. The foam anvils were placed on a steel frame which supported an adjustable ramp (Fig. 6). The ramp was also adjustable between 0° and 30° with increments of 5° and secured rigidly in place. Overall, between the adjustable ramp and the frame, this provided an effective angle range between 0° and 60°. A photoelectric time gate was attached to the frame just before the stopper to measure the velocity. There was a significant height difference between where the headform was released and the impact location on the anvil. As a result, the inbound velocity of the headform at impact was calculated using projectile motion equations and the velocity measured from the photoelectric time gate.

A range of vinyl nitrile (VN) foams was used to serve as representative anvils for different levels of surface compliance in the reconstructions. In Ireland and Britain, a 7-point Going Rating scale ranging from Heavy to Hard is used as a descriptive measurement to determine whether a racetrack is suitable for racing without a risk of injury to a horse. Separate work<sup>23</sup> has examined the relationship between Going Rating and kinematic response characteristics and determined that the 7-point Going Rating scale could be simplified with a 3-point scale without any loss of biomechanical accuracy. Three representative anvils were subsequently developed and represent these three points, namely Soft (H–S), Good (GS–GF), and Firm (F–H). The anvil for the Soft condition consisted of 95 mm of Monarch F-06231 (Armacell Canada Inc., Brampton, ON). Hardness for Monarch F-06231 foam was Shore 00 of 50–60. The Good and Firm conditions were represented by anvils consisting of 66 mm VN 602 and 74 mm VN 704, respectively (DER-TEX Corporation, Saco, ME). Hardness for the VN 602 and VN 704 foam were Shore 00 of 45–65 and Shore 00 of 65–85, respectively. The foam anvils were covered either with SYNGrass UltraLush™ 40 (synthetic grass) to represent a turf surface or double-sided tape covered with sand to represent a sand surface. Since the Going Rating for sand is not measured for all impacts to sand, the Good anvil was selected, as this was the mid-range compliance from the three developed anvils. Impacts to turf and sand have previously been found to have similar head kinematics and brain tissue response for drop tests<sup>23</sup> and therefore, the mid-range for compliance was deemed the most suitable from the three developed anvils to represent sand impacts.

The finite element model used in this study is the University College Dublin Brain Trauma Model (UCDBTM).<sup>24,25</sup> The geometry of the UCDBTM was derived from computed tomography

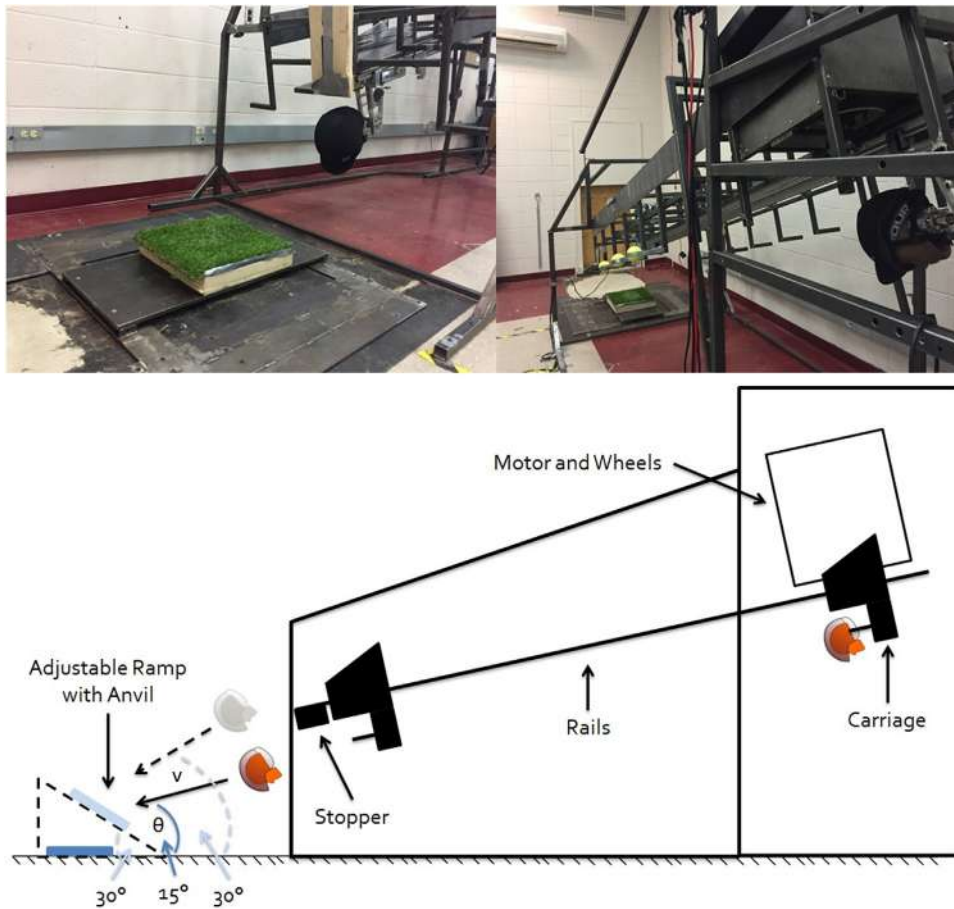


Fig. 6. Photographs of rail guided launcher with Hybrid III headform attached to the carriage on the top and a simplified schematic of rail guided launcher on the bottom.

Table 1  
 Material properties of UCDBTM.

Material	Young's modulus (MPa)	Density (kg/m <sup>3</sup> )	Poisson's ratio
Scalp	16.7	1000	0.42
Cortical bone	15000	2000	0.22
Trabecular bone	1000	1300	0.24
Dura	31.5	1130	0.45
Pia	11.5	1130	0.45
Falx	31.5	1140	0.45
Tentorium	31.5	1140	0.45
CSF	Water	1000	0.5
Grey matter	Viscoelastic	1060	0.49

Table 2  
 Material characteristics of the brain tissue for the UCDBTM.

Material	G <sub>0</sub>	G <sub>∞</sub>	Bulk modulus (GPa)	Decay constant (s <sup>-1</sup> )
Cerebellum	10	2	2.19	80
Brain stem	22.5	4.5	2.19	80
White matter	12.5	2.5	2.19	80
Grey matter	10	2	2.19	80

(CT) and magnetic resonance imaging scans (MRI) of a male human cadaver.<sup>24</sup> The three-dimensional finite element model consists of the scalp, skull, pia, falx, tentorium, cerebrospinal fluid (CSF), grey and white matter, cerebellum and brain stem, represented by approximately 26,000 elements.<sup>24,25</sup> Subsequent modifications were performed on the UCDBTM to increase mesh density and introduce bridging veins. The material characteristics of the UCDBTM were taken from the literature and are presented in Tables 1 and 2. Validation of the UCDBTM was performed against

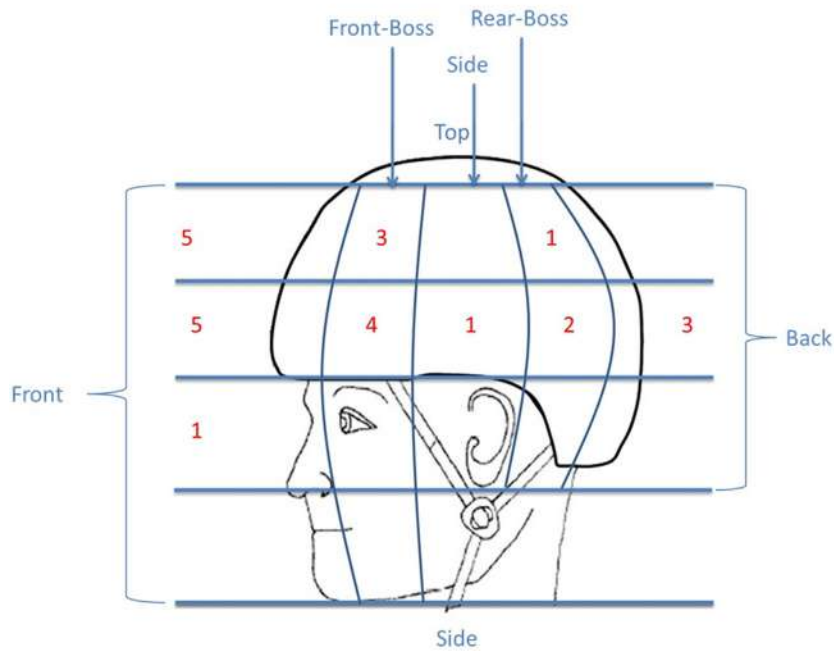
intracranial pressure response and brain motion response of previous cadaver research.

Impact parameters (impact velocity and trajectory angle), peak resultant head kinematics (linear acceleration rotational acceleration, rotational velocity and impact duration) and brain tissue response (MPS, VMS and CSDM<sub>10</sub>) were used to compare concussive and non-concussive falls in equestrian sports. Independent sample t-tests were used to determine if there were significant differences between the results for concussive and non-concussive cases. Binary logistic regressions were used to examine which variables could successfully distinguish between concussive and non-concussive cases. Additionally, Pearson correlation coefficients (r) and R<sup>2</sup> values were calculated to determine how head kinematics correlated to brain tissue response. A significance level of  $\alpha = 0.05$  was used for all statistical tests. The statistical software package used for this study was of SPSS 24.0 for Windows (SPSS Inc., Chicago, IL, USA).

### 3. Results

In total, 25 concussive and 25 non-concussive cases met the inclusion criteria of the study and were subsequently reconstructed. Descriptions and results for each of the reconstructed cases are presented in the Appendix. Twenty-three concussive and 23 non-concussive cases were as a result of horse racing accidents. Two concussive and two non-concussive cases occurred in the cross-country phase of eventing. Forty-three of the cases involved male jockeys while seven involved female jockeys. Impact locations for both concussive and non-concussive cases are shown in Fig. 7. Concussive impacts occurring to the front or front-boss region of

## Concussive (n = 25)



## Non-Concussive (n = 25)

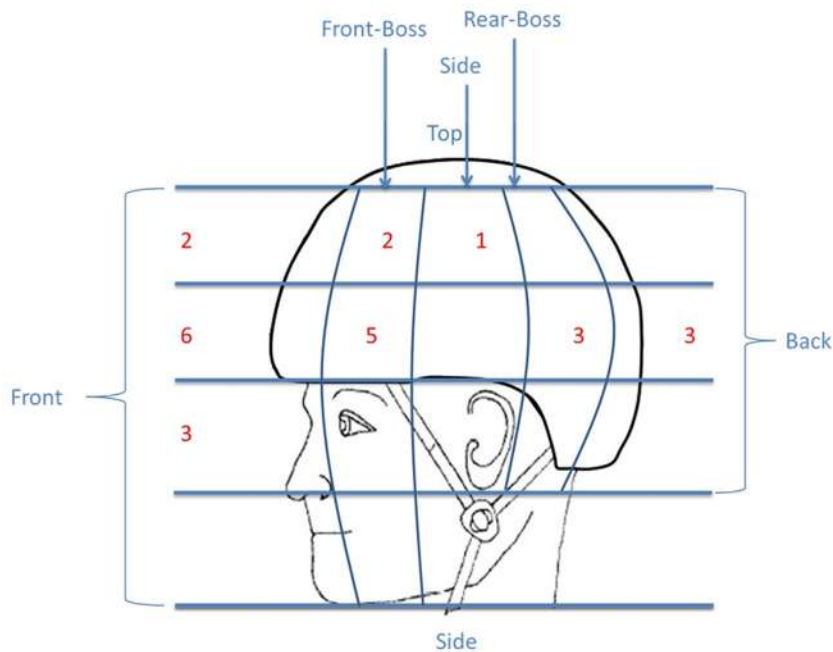


**Fig. 7.** Concussive and non-concussive impact locations for real-world accident reconstructions in equestrian sports. Note that images collate cases from both the left and right side of the sagittal plane.

the head represented 72% of the concussive cases. Impact locations for non-concussive cases were matched as closely as possible to concussive cases. Table 3 presents the distribution of cases to sand surfaces and Going Rating on a three-point scale. The majority of the accidents occurred on turf surfaces with Going rating of Good (GS-GF), with a smaller number being Soft (HS), or against sand. No accidents occurred when the Going Rating was Firm (FH). The

distribution of impacts to sand surfaces and Going Rating on the three-point scale was similar for concussive and non-concussive cases.

The results of the independent sample t-tests show that concussive cases had significantly greater impact velocity, linear acceleration, rotational acceleration, rotational velocity, MPS, VMS and CSDM<sub>10</sub> than non-concussive cases ( $p < 0.05$ ). There was no sig-

**Table 3**  
Distribution of impacts to sand surfaces and a three-point Going Rating scaling for concussive and non-concussive cases.

Anvil	Non-concussive	Concussive
Soft (HS)	6	5
Good (GS-GF)	17	16
Firm (FH)	0	0
Sand	2	4

**Table 4**  
Mean reconstruction results ( $\pm 1$  standard deviation) for 25 concussive and 25 non-concussive falls in equestrian sports. Dependant variables which result in statistically significant differences between concussion and non-concussive cases are indicate with an\*.

Variable	Non-concussive	Concussive
Impact velocity (m/s)*	7.4 (2.4)	10.1 (2.9)
Trajectory angle (°)	28 (12)	28 (15)
Linear acceleration (g)*	53.2 (25.0)	65.7 (25.3)
Rotational acceleration (rad/s <sup>2</sup> )*	2245 (1158)	3372 (1995)
Rotational velocity (rad/s)*	22.9 (9.8)	35.2 (18.1)
Impact duration (ms)	26.6 (2.9)	27.4 (3.5)
Maximum principal strain*	0.199 (0.107)	0.305 (0.177)
von Mises Stress (kPa)*	10.1 (5.4)	8.5 (5.7)
CSDM <sub>10</sub> *	0.175 (0.255)	0.375 (0.371)

nificant difference between concussive and non-concussive cases for trajectory angle and impact duration ( $p > 0.05$ ). The results for concussive and non-concussive cases are presented in Table 4.

Binary logistic regression analysis revealed that impact velocity, linear acceleration, rotational acceleration, rotational velocity, MPS, VMS and CSDM<sub>10</sub> were significant predictors of concussion ( $p < 0.05$ ). Trajectory angle and impact duration were found not to be significant predictors of concussion ( $p > 0.05$ ). Impact velocity had the largest percent correct classification at 70% and the other significant predictors had similar predictive capabilities to one another (60.0–64.7%). The results of the binary logistic regressions along with the percentile risk classification are presented in Table 5.

Pearson correlations were conducted on the entire dataset and concussive and non-concussive cases were separated to determine the relationship between head kinematics and brain tissue response (Table 6 and Figs. 8–10). All correlations between head kinematics and brain tissue response were found to be signif-

icant ( $p < 0.01$ ). Rotational acceleration was found to have the strongest correlation with brain tissue response ( $r > 0.920$ ), closely followed by rotational velocity ( $r > 0.840$ ). These strong correlations were consistent across all datasets (i.e. all, non-concussive and concussive). Linear acceleration had moderate to very weak correlations with brain tissue response ( $r = 0.306–0.735$ ). The correlations decrease across datasets in which the non-concussive cases had the highest correlations between linear acceleration and brain tissue response, followed by all cases grouped together, and with the concussive cases having the weakest correlations. Moderate correlations were found for the non-concussive events.

#### 4. Discussion

The purpose of this study was to investigate the biomechanics of real-world accidents in equestrian sports and develop thresholds for concussive injury. The head kinematics and brain tissue thresholds for concussion in equestrian sports was found to be within the range of concussive thresholds previously identified for other sports.<sup>15,27,28</sup> Despite similarities with reported head kinematic concussive thresholds in literature, a unique combination of concussive head kinematic thresholds that are specific to equestrian sports was found. Rotational velocity thresholds were similar to those reported for American football and Australian rules football and rugby, while the linear acceleration threshold was at the lower end of reported thresholds. Compared to concussive thresholds for ice hockey collisions, the linear acceleration threshold of this study was higher but the rotational acceleration threshold was similar. The unique combination of head kinematics is a direct consequence of equestrian head impacts being an oblique fall to a compliant surface which is not represented in other datasets in the literature. As such, these 50 reconstructed equestrian accidents constitute an important contribution to the growing body of real-world head injury accidents. The low magnitude rotational accelerations and long durations ( $> 20$  ms) are a reflection of the compliant impact surfaces, whereas the relatively high magnitude linear accelerations for the given impact duration were a reflection of the large amount of energy transferred to the head during falls.

While the head kinematic thresholds varied from those reported elsewhere in the literature, concussive brain tissue response thresholds obtained in this study were consistent across sports.<sup>16,17,29</sup> These results support the hypothesis that differ-

**Table 5**  
Binary logistic regression results for concussive and non-concussive falls in equestrian sports.

Variable	-2 log Likelihood ratio	p value	Nagelkerke R <sup>2</sup>	Percent correct classification	Concussion likelihood
Impact velocity	57.5	0.004	0.281	70.0	7.5 m/s for 25% 8.7 m/s for 50% 10.2 m/s for 80%
Trajectory angle	69.3	0.829	0.001	48.0	NA
Linear acceleration	198.7	0.004	0.080	64.0	36 g for 25% 59 g for 50% 89 g for 80%
Rotational acceleration	190.0	0.001	0.151	60.0	1700 rad/s <sup>2</sup> for 25% 2700 rad/s <sup>2</sup> for 50% 4000 rad/s <sup>2</sup> for 80%
Rotational velocity	182.4	0.001	0.209	64.7	21 rad/s for 25% 28 rad/s for 50% 38 rad/s for 80%
Impact duration	205.1	0.096	0.025	58.7	NA
Maximum principal strain	188.5	0.001	0.162	60.7	0.15 for 25% 0.24 for 50% 0.36 for 80%
von Mises Stress	190.5	0.001	0.146	62.7	3.9 kPa for 25% 6.6 kPa for 50% 10.0 kPa for 80%
CSDM <sub>10</sub>	193.6	0.001	0.121	60.7	0.02 for 25% 0.27 for 50% 0.57 for 80%



**Table 6**  
 Pearson correlations for head kinematics to maximum principal strain of real-world accident reconstructions in equestrian sports.

Dataset	Comparison	Pearson Correlation (r)	R <sup>2</sup>
All	Linear acceleration/MPS	0.495 <sup>a</sup>	0.245
	Rotational acceleration/MPS	0.982 <sup>a</sup>	0.964
	Rotational velocity/MPS	0.933 <sup>a</sup>	0.870
	Linear acceleration/VMS	0.469 <sup>a</sup>	0.220
	Rotational acceleration/VMS	0.984 <sup>a</sup>	0.968
	Rotational velocity/VMS	0.898 <sup>a</sup>	0.806
	Linear acceleration/CSDM <sub>10</sub>	0.524 <sup>a</sup>	0.247
	Rotational acceleration/CSDM <sub>10</sub>	0.932 <sup>a</sup>	0.869
	Rotational velocity/CSDM <sub>10</sub>	0.892 <sup>a</sup>	0.796
	Linear acceleration/MPS	0.699 <sup>a</sup>	0.489
Non-concussive	Rotational acceleration/MPS	0.977 <sup>a</sup>	0.954
	Rotational velocity/MPS	0.892 <sup>a</sup>	0.796
	Linear acceleration/VMS	0.735 <sup>a</sup>	0.540
	Rotational acceleration/VMS	0.974 <sup>a</sup>	0.949
	Rotational velocity/VMS	0.847 <sup>a</sup>	0.717
	Linear acceleration/CSDM <sub>10</sub>	0.688 <sup>a</sup>	0.473
	Rotational acceleration/CSDM <sub>10</sub>	0.926 <sup>a</sup>	0.857
	Rotational velocity/CSDM <sub>10</sub>	0.864 <sup>a</sup>	0.746
	Linear acceleration/MPS	0.322 <sup>a</sup>	0.104
	Rotational acceleration/MPS	0.977 <sup>a</sup>	0.954
Concussive	Rotational velocity/MPS	0.892 <sup>a</sup>	0.796
	Linear acceleration/VMS	0.306 <sup>a</sup>	0.094
	Rotational acceleration/VMS	0.988 <sup>a</sup>	0.976
	Rotational velocity/VMS	0.898 <sup>a</sup>	0.806
	Linear acceleration/CSDM <sub>10</sub>	0.377 <sup>a</sup>	0.142
	Rotational acceleration/CSDM <sub>10</sub>	0.928 <sup>a</sup>	0.861
	Rotational velocity/CSDM <sub>10</sub>	0.895 <sup>a</sup>	0.801

<sup>a</sup> Correlation is significant at the 0.01 level (2-tailed).

ent impact events with different magnitude and duration of head kinematics can result in concussion. This is consistent with the fundamental view that brain tissue response measures are a suitable basis for injury threshold criteria that can apply regardless of the cause of a head impact or either the magnitude or duration of an impact event. Finite element modelling accounts for the interaction between different types of acceleration curve shapes, whilst using peak head kinematics alone can lead to discrepancies when comparing values collected for different impact event types.

As expected, concussive cases were associated with higher impact velocities, peak head kinematics and brain tissue response values than non-concussive impacts. Clearly, for all else being equal, faster impact velocities result in higher head kinematics and brain tissue responses and subsequently increase the risk of injury. It was also unsurprising that impact velocity was found to be the best predictor of concussion. Impact velocity represents the fundamental difference between concussive and non-concussive cases, as greater levels of impact energy correspond to greater risks of concussion and, therefore, lowering impact velocity can help to reduce the risk of concussion. While decreasing impact velocity may not be a practical design solution for equestrian sports and horse racing, pre-impact movements to reduce the impact velocity and acceleration in trained fall techniques are often taught in combat sports and gymnastics as injury prevention strategies, although falls in equestrian sports do not always allow riders sufficient reaction time before impact.<sup>30</sup> Further management of impact velocity in eventing could be achieved by modifying the rules for course completion times.

The results of this study also have significant implications for equestrian helmet standards and helmet designs. Concussive accidents in equestrian sports were associated with an oblique impact to a compliant surface. These types of impact resulted in considerably lower accelerations (<130 g) than the commonly used 250 g threshold in current equestrian standards that involves a linear drop to a steel surface.<sup>9–11</sup> The concussive accidents also had considerably longer impact durations than current equestrian hel-

met standard impacts, which are less than 15 ms in duration. This indicates that the current equestrian helmet standards and design tests do not properly account for the loading conditions associated with concussion. Consequently, the performance of equestrian helmets under real-world accident loading conditions is currently unknown. Future work should aim to assess the protective capacity of equestrian helmets for oblique impacts to a compliant anvil and the use of appropriate injury threshold values similar to those reported in this study when assessing the risk of concussion (Table 5). Additionally, in this study, rotational kinematics were found to be strongly correlated to MPS for concussion, whereas linear acceleration had a very weak correlation. By assessing the protective capacity of equestrian helmets for the loading conditions associated with concussion and traumatic brain injury, it will be possible to improve helmet designs and reduce the occurrence of brain injury in equestrian sports.

The methodology of this research involved reconstructions of filmed accidents in competition in which injury classification was dependent on diagnosis by a medical doctor. Concussion can be a somewhat subjective diagnosis based upon observed symptoms and it is possible that some riders may have been misdiagnosed as a false positive or false negative. The reconstructions were conducted using the best estimates from video analysis but there is some inherent variation in the estimated independent variables (i.e., displacement and velocity) for each individual impact. Furthermore, the Hybrid III headforms are commonly used in accident reconstructions<sup>13</sup> but may not imitate the exact response of the human head, but rather they provide an approximation of human response. This limitation also applies to the response of the UCDBTM as it is dependent on the assigned material properties.

## 5. Conclusion

Concussive cases are found to have significantly higher impact velocities, peak head kinematics and brain tissue response val-

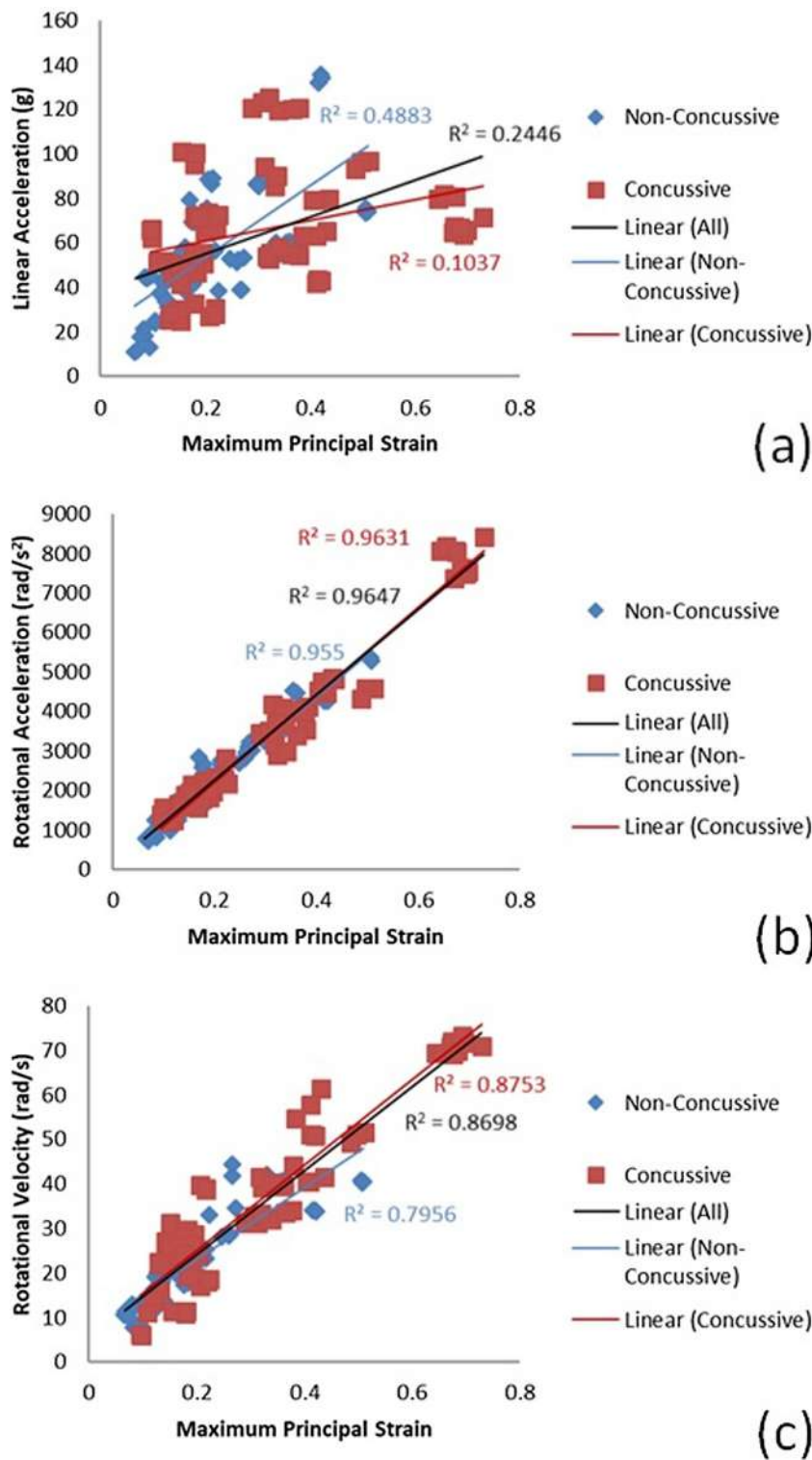


**Fig. 8.** Scatterplots showing the relationship between head kinematics and maximum principal strain (MPS) for real-world reconstructions of concussive and non-concussive cases in equestrian sports: (a) linear acceleration/MPS, (b) rotational acceleration/MPS and (c) rotational velocity/MPS.

ues than non-concussive impacts. Thresholds for a 50% risk of concussion have been established in terms of linear and angular acceleration, maximum principal strain, Von Mises stress and cumulative strain damage [59 g, 2700 rad/s<sup>2</sup>, 28 rad/s, 0.24 (MPS), 6.6 kPa and 0.27 (CSMD<sub>10</sub>)]. These are within the range of concussive thresholds reported in the literature and they represent

a distinctly different combination of head kinematic thresholds compared to other sports.

From the accident reconstructions, it is apparent that current certification standards for equestrian helmets represent different loading conditions than those associated with real-world concussion. Current standards commonly use a threshold of 250 g and a

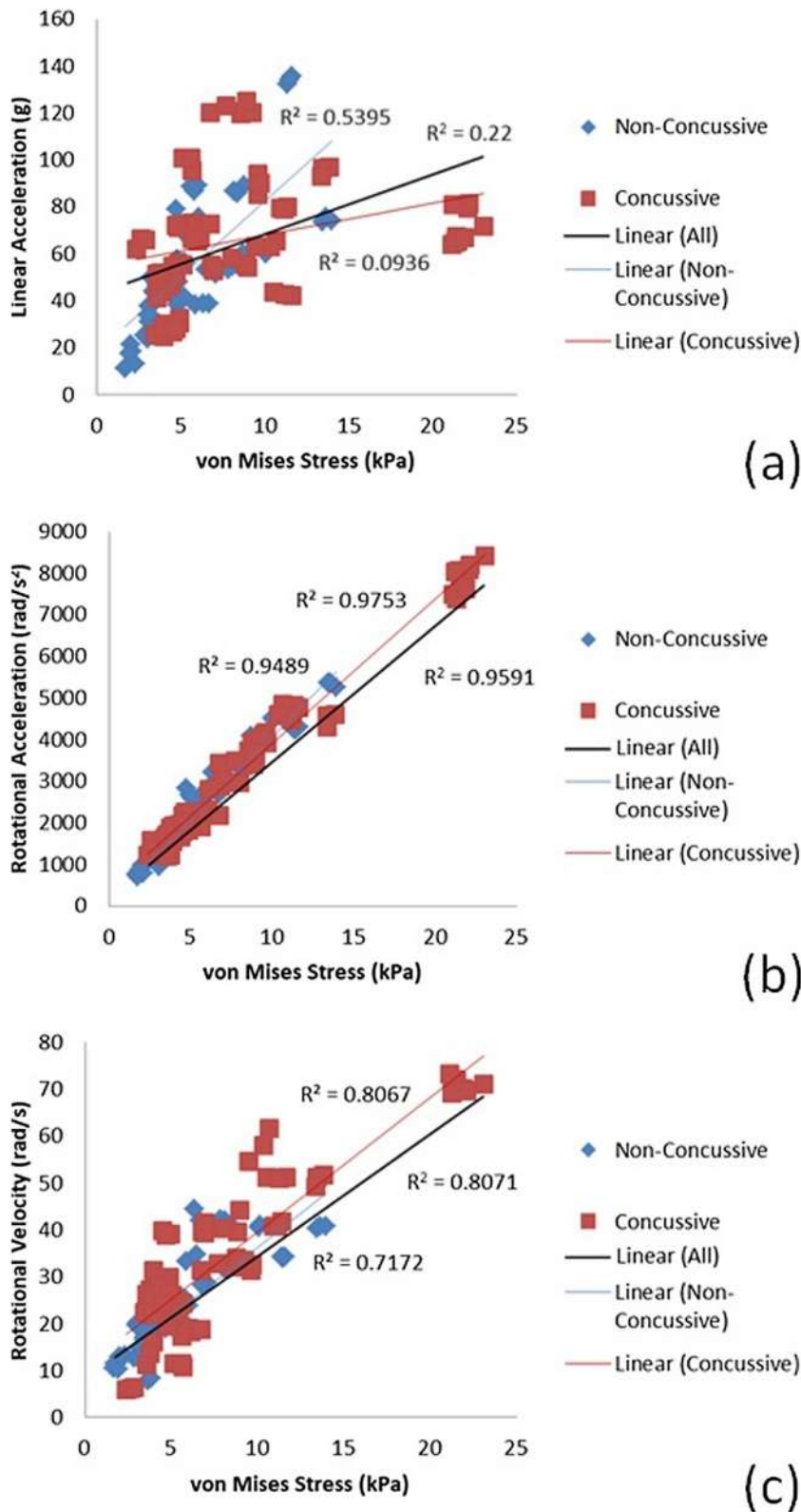


**Fig. 9.** Scatterplots showing the relationship between head kinematics and von Miss stress (VMS) for real-world reconstructions of concussive and non-concussive cases in equestrian sports: (a) linear acceleration/VMS, (b) rotational acceleration/VMS and (c) rotational velocity/VMS.

linear drop to a steel anvil that results in short duration impacts (less than 15 ms), whereas concussive equestrian accidents occur from oblique impacts to turf or sand, resulting in lower magnitude and longer duration impacts (<130 g and >20 ms, respectively). It is

unknown how equestrian helmets perform for oblique impacts to a compliant surface and, therefore, there is a need to assess the protective capacity of equestrian helmets under these impact loading conditions.

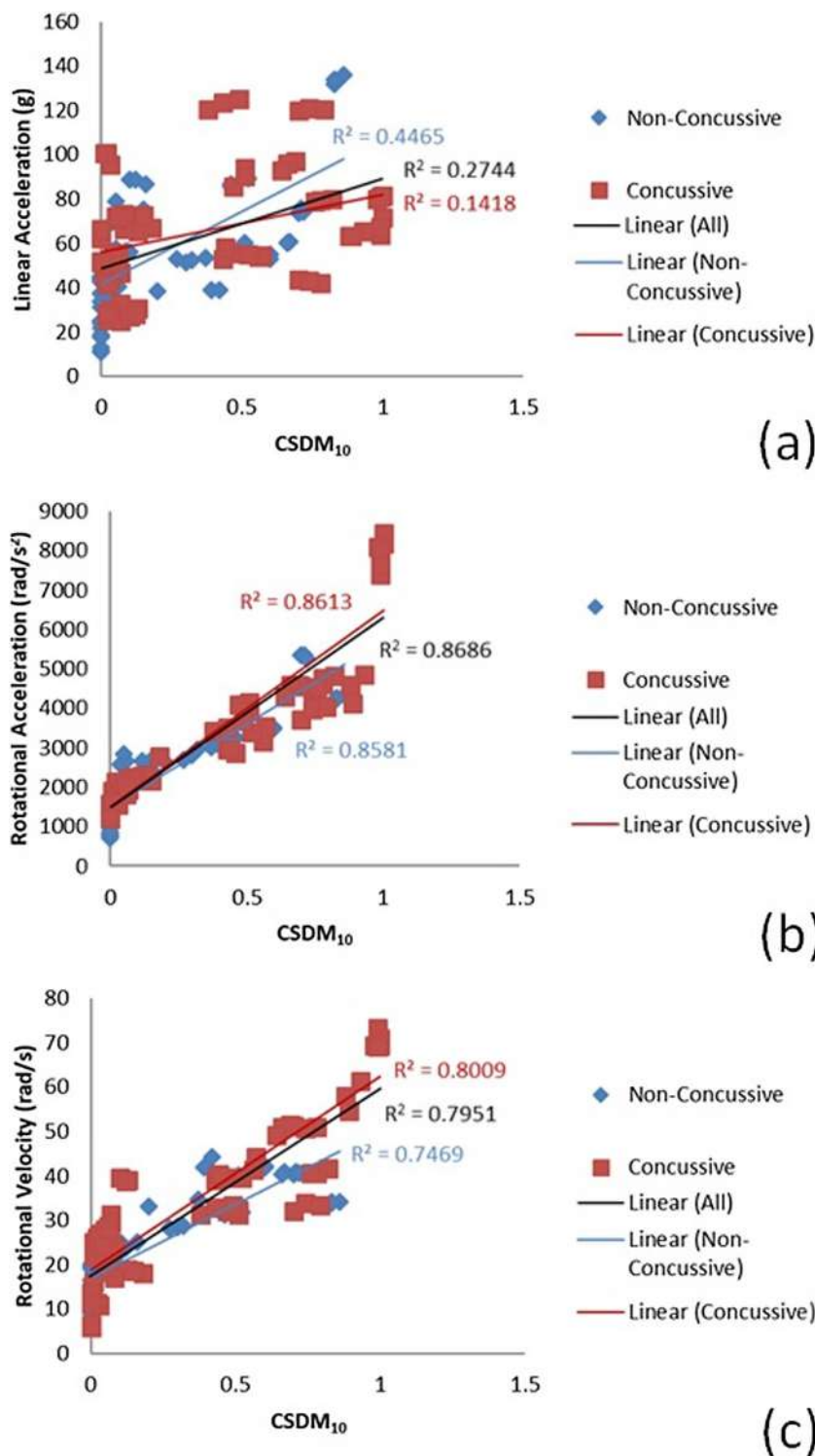


**Fig. 10.** Scatterplots showing the relationship between head kinematics and cumulative strain damage measure 10% (CSDM<sub>10</sub>) for real-world reconstructions of concussive and non-concussive cases in equestrian sports: (a) linear acceleration/CSDM<sub>10</sub>, (b) rotational acceleration/CSDM<sub>10</sub> and (c) rotational velocity/CSDM<sub>10</sub>.

**Acknowledgements**

This research received funding from the European Union’s Horizon 2020 research and innovation programme under the Marie Skłodowska-Curie grant agreement No. 642662. Helmets for this work were supplied by Charles Owen.

**Appendix A.**

This appendix presents the descriptions and reconstruction results for each case in this study. The data accidents occurring in the cross-country phase of eventing are presented in Tables A1 and A2. Tables A3 and A4 present data relating to accidents occurring in horse racing. Corresponding video footage of each accident case are available from the Corresponding Author upon request.



**Table A1**  
Accident descriptions and impact parameters for reconstructed cases in eventing.

ID	Sex	Discipline	Surface Type	Ground Conditions	Injury	Impact Location	Impact Velocity				Trajectory Angle (°)
							Resultant	x	y	z	
E-1	Female	Cross-Country	Turf	Good	Concussion	R4	7.51	0.09	6.19	-4.24	34
E-2	Female	Cross-Country	Turf	Good	None	L4	2.47	0.23	2.26	-0.99	23
E-3	Female	Cross-Country	Turf	Good-Soft	Concussion	B2	6.74	0.23	4.59	-4.93	47
E-4	Female	Cross-Country	Turf	Good	None	B2	4.95	-0.45	2.33	-4.34	61

**Table A2**  
Mean reconstruction results ( $\pm 1$  standard deviation) for each eventing case.

ID	Linear Acceleration (g)	Rotational Acceleration (rad/s <sup>2</sup> )	Rotational Velocity (rad/s)	Impact Duration (ms)	Maximum Principal Strain	von Mises Stress (kPa)	CSDM <sub>10</sub>
E-1	72.5 (0.7)	2084 (91)	23.2 (0.9)	24.7 (0.2)	0.192 (0.013)	5.3 (0.5)	0.063 (0.015)
E-2	11.9 (1.0)	845 (176)	11.7 (1.3)	25.7 (1.0)	0.076 (0.015)	1.9 (0.3)	0.000 (0.000)
E-3	74.0 (4.8)	2702 (134)	21.3 (2.2)	23.9 (0.4)	0.174 (0.004)	4.9 (0.2)	0.050 (0.010)
E-4	64.7 (2.3)	1396 (179)	6.1 (0.2)	24.5 (0.3)	0.097 (0.002)	2.6 (0.3)	0.000 (0.000)

**Table A3**  
Accident descriptions and impact parameters for reconstructed cases in horse racing.

ID	Sex	Discipline	Surface Type	Ground Conditions	Injury	Impact Location	Impact Velocity				Trajectory Angle (°)
							Resultant	x	y	z	
R-1	Male	Jump	Turf	Good	None	L2	8.47	0.11	7.42	-4.08	29
R-2	Male	Flat	Sand	NA	Concussion	F2	9.99	-0.15	9.60	-2.75	16
R-3	Male	Jump	Turf	Heavy	Concussion	F3	7.81	0.09	3.44	-7.01	64
R-4	Male	Jump	Turf	Soft	Concussion	L1	9.01	0.03	8.22	-3.68	24
R-5	Male	Jump	Turf	Good-Soft	None	L4	8.32	0.12	7.69	-3.17	22
R-6	Male	Jump	Turf	Good	Concussion	F1	10.32	0.01	9.34	-4.40	25
R-7	Female	Jump	Turf	Good	Concussion	R4	10.82	-0.29	10.49	-2.60	14
R-8	Male	Jump	Turf	Good	None	F2	7.63	0.13	6.95	-3.14	24
R-9	Male	Jump	Turf	Soft	None	F2	5.32	-0.55	4.63	-2.56	29
R-10	Male	Jump	Turf	Soft	None	B2	8.47	1.12	6.10	-5.77	43
R-11	Male	Jump	Turf	Soft	None	F3	3.93	0.02	3.66	-1.41	21
R-12	Male	Jump	Turf	Good	Concussion	R1	9.68	-0.12	8.55	-4.54	28
R-13	Male	Flat	Turf	Good-Firm	Concussion	R6	13.84	-0.04	12.70	-5.51	23
R-14	Male	Jump	Turf	Heavy	Concussion	R3	9.36	0.87	6.64	-6.53	44
R-15	Male	Jump	Turf	Good	None	L1	7.72	0.28	7.18	-2.83	21
R-16	Male	Jump	Turf	Soft	None	L4	6.85	-0.93	6.39	-2.28	19
R-17	Male	Jump	Turf	Good	Concussion	F2	9.74	0.41	9.10	-3.43	21
R-18	Male	Jump	Turf	Good-Soft	None	F1	11.11	-0.03	10.77	-2.73	14
R-19	Male	Flat	Sand	NA	Concussion	R4	15.24	-0.06	14.81	-3.60	14
R-20	Male	Flat	Sand	NA	None	B2	11.81	-0.86	7.46	-9.12	51
R-21	Female	Jump	Turf	Good	Concussion	F1	6.58	0.11	6.08	-2.52	22
R-22	Male	Jump	Turf	Soft	None	F3	7.25	-0.10	7.06	-1.64	13
R-23	Male	Jump	Turf	Good	None	F2	6.40	-0.22	5.87	-2.53	23
R-24	Male	Jump	Turf	Good	Concussion	B2	10.58	1.17	7.61	-7.25	43
R-25	Male	Flat	Sand	NA	Concussion	F1	13.32	0.14	12.74	-3.88	17
R-26	Male	Flat	Sand	NA	Concussion	B2	11.20	-0.20	7.70	-8.12	47
R-27	Female	Jump	Turf	Good	Concussion	F1	11.56	-0.02	11.38	-2.01	10
R-28	Male	Jump	Turf	Good-Soft	None	R6	3.80	0.45	2.15	-3.11	55
R-29	Male	Jump	Turf	Good-Soft	Concussion	F2	7.70	0.14	6.92	-3.37	26
R-30	Male	Jump	Turf	Good	Concussion	L1	13.21	0.08	12.36	-4.66	21
R-31	Male	Jump	Turf	Good	Concussion	L4	6.28	0.16	4.57	-4.31	43
R-32	Male	Jump	Turf	Soft	Concussion	L5	7.13	-0.59	6.13	-3.59	30
R-33	Male	Jump	Turf	Good	None	L4	6.81	-0.51	5.96	-3.26	29
R-34	Male	Jump	Turf	Good	Concussion	R6	7.02	0.07	5.53	-4.32	38
R-35	Male	Jump	Turf	Good	None	R6	9.15	-0.04	8.56	-3.24	21
R-36	Male	Jump	Turf	Good	None	F3	3.39	0.15	3.14	-1.28	22
R-37	Male	Jump	Turf	Good	None	R1	9.75	-0.06	9.19	-3.28	20
R-38	Male	Flat	Sand	NA	None	F2	9.05	-1.03	8.27	-3.55	23
R-39	Male	Flat	Sand	NA	Concussion	F2	16.24	0.05	15.46	-4.98	18
R-40	Male	Jump	Turf	Good	None	R6	11.21	-0.46	10.80	-2.96	15
R-41	Male	Jump	Turf	Good	None	R4	7.00	0.52	6.55	-2.41	20
R-42	Male	Jump	Turf	Good-Soft	None	F2	6.54	0.28	4.54	-4.70	46
R-43	Male	Flat	Sand	NA	Concussion	F1	11.59	0.06	11.28	-2.70	13
R-44	Male	Jump	Turf	Good	Concussion	F2	11.64	0.09	11.16	-3.31	17
R-45	Male	Jump	Turf	Good	None	F2	9.00	0.33	7.54	-4.91	33
R-46	Male	Jump	Turf	Soft	None	F1	7.37	-0.10	6.39	-3.67	30

**Table A4**  
Mean reconstruction results ( $\pm 1$  standard deviation) for each horse racing case.

ID	Linear Acceleration (g)	Rotational Acceleration (rad/s <sup>2</sup> )	Rotational Velocity (rad/s)	Impact Duration (ms)	Maximum Principal Strain	von Mises Stress (kPa)	CSDM <sub>10</sub>
R-1	74.4 (1.2)	5328 (49)	40.6 (0.3)	24.1 (0.1)	0.507 (0.002)	13.7 (0.3)	0.710 (0.010)
R-2	42.9 (0.8)	4602 (147)	51.0 (0.2)	30.7 (0.5)	0.415 (0.004)	11.1 (0.60)	0.740 (0.040)
R-3	98.9 (3.0)	2046 (117)	11.2 (0.3)	23.2 (0.3)	0.171 (0.014)	5.5 (0.3)	0.020 (0.010)
R-4	54.0 (1.3)	3001 (142)	40.1 (1.2)	29.5 (0.6)	0.321 (0.003)	6.9 (0.1)	0.483 (0.068)
R-5	49.1 (1.0)	1713 (26)	13.3 (1.1)	24.6 (0.5)	0.132 (0.009)	3.5 (0.3)	0.007 (0.006)
R-6	55.9 (2.1)	3306 (297)	41.4 (2.5)	30.4 (1.0)	0.360 (0.019)	8.6 (0.5)	0.510 (0.066)
R-7	46.1 (1.4)	1683 (29)	23.6 (1.7)	29.7 (0.3)	0.144 (0.007)	4.0 (0.4)	0.013 (0.006)
R-8	55.9 (0.8)	2237 (82)	22.7 (2.8)	26.7 (0.2)	0.212 (0.010)	5.1 (0.1)	0.083 (0.021)
R-9	43.2 (0.8)	1239 (75)	15.8 (0.5)	27.8 (0.5)	0.120 (0.002)	3.6 (0.2)	0.000 (0.000)
R-10	88.1 (1.3)	2586 (234)	23.8 (1.2)	25.3 (0.3)	0.210 (0.004)	5.8 (0.2)	0.127 (0.031)
R-11	24.7 (0.8)	1182 (124)	12.7 (0.3)	30.8 (1.2)	0.110 (0.011)	3.1 (0.3)	0.000 (0.000)
R-12	79.4 (0.4)	4656 (145)	40.9 (0.6)	24.7 (0.3)	0.417 (0.017)	11.1 (0.2)	0.787 (0.031)
R-13	95.4 (2.1)	4497 (162)	50.6 (1.2)	24.9 (0.2)	0.499 (0.013)	13.5 (0.3)	0.663 (0.025)
R-14	89.9 (4.3)	4064 (118)	31.9 (0.6)	25.4 (0.5)	0.327 (0.013)	9.6 (0.0)	0.497 (0.023)
R-15	38.8 (1.1)	1854 (113)	21.3 (1.2)	29.8 (0.4)	0.164 (0.004)	4.9 (0.1)	0.040 (0.010)
R-16	37.4 (0.2)	1038 (60)	13.5 (1.2)	31.6 (0.2)	0.115 (0.001)	3.1 (0.0)	0.000 (0.000)
R-17	50.3 (0.3)	1814 (229)	27.5 (1.5)	29.0 (0.3)	0.181 (0.014)	4.3 (0.4)	0.047 (0.015)
R-18	38.7 (0.3)	3000 (292)	39.7 (5.9)	28.2 (0.1)	0.253 (0.025)	6.3 (0.4)	0.337 (0.119)
R-19	65.7 (1.8)	7708 (320)	72.3 (0.8)	29.2 (0.1)	0.688 (0.013)	21.4 (0.2)	0.990 (0.000)
R-20	133.9 (1.9)	4276 (35)	34.1 (0.2)	20.1 (0.1)	0.420 (0.003)	11.5 (0.1)	0.840 (0.017)
R-21	30.2 (2.3)	1888 (305)	25.7 (3.9)	31.4 (0.8)	0.153 (0.024)	4.3 (0.5)	0.040 (0.026)
R-22	33.0 (1.6)	1343 (84)	19.6 (0.5)	32.7 (1.1)	0.127 (0.002)	3.1 (0.1)	0.000 (0.000)
R-23	47.6 (1.0)	1604 (63)	19.3 (1.2)	26.7 (0.1)	0.141 (0.010)	4.0 (0.4)	0.020 (0.010)
R-24	120.2 (0.6)	3907 (162)	33.2 (1.0)	20.9 (0.2)	0.360 (0.020)	8.9 (0.3)	0.743 (0.045)
R-25	67.9 (3.4)	7818 (545)	70.7 (0.6)	29.9 (0.1)	0.695 (0.030)	22.1 (0.9)	0.993 (0.006)
R-26	122.8 (2.4)	3546 (135)	32.5 (1.0)	21.5 (0.2)	0.306 (0.016)	7.8 (1.1)	0.433 (0.055)
R-27	25.3 (0.3)	1826 (147)	26.9 (4.5)	30.4 (0.4)	0.141 (0.011)	3.7 (0.3)	0.043 (0.025)
R-28	44.7 (0.6)	1342 (92)	8.0 (0.2)	23.0 (0.2)	0.090 (0.006)	3.7 (0.1)	0.000 (0.000)
R-29	55.2 (0.4)	1862 (88)	25.5 (1.2)	27.3 (0.4)	0.164 (0.004)	4.8 (0.3)	0.053 (0.012)
R-30	64.0 (1.3)	4528 (374)	58.0 (3.4)	27.4 (0.4)	0.409 (0.023)	10.2 (0.6)	0.900 (0.026)
R-31	66.3 (0.7)	2458 (297)	18.0 (0.9)	24.3 (1.2)	0.209 (0.011)	5.9 (0.3)	0.130 (0.050)
R-32	51.3 (0.5)	1342 (221)	13.6 (2.5)	27.9 (0.6)	0.121 (0.012)	3.8 (0.2)	0.003 (0.006)
R-33	56.3 (1.5)	1930 (118)	22.0 (1.2)	25.2 (0.3)	0.163 (0.010)	4.9 (0.2)	0.050 (0.010)
R-34	71.7 (0.8)	2081 (78)	19.1 (0.4)	24.4 (0.1)	0.199 (0.023)	5.5 (1.1)	0.087 (0.055)
R-35	48.0 (0.6)	1696 (40)	23.1 (1.8)	27.6 (0.4)	0.163 (0.023)	4.3 (0.4)	0.033 (0.015)
R-36	19.3 (2.1)	881 (97)	11.9 (1.5)	29.5 (1.1)	0.081 (0.005)	2.0 (0.1)	0.000 (0.000)
R-37	53.8 (1.0)	3335 (284)	39.6 (4.3)	25.7 (0.6)	0.312 (0.033)	7.5 (0.9)	0.523 (0.133)
R-38	60.4 (0.2)	4356 (230)	40.5 (0.5)	27.1 (0.4)	0.351 (0.014)	9.6 (0.8)	0.613 (0.090)
R-39	80.7 (1.0)	8107 (72)	69.3 (0.2)	28.7 (0.4)	0.658 (0.014)	21.8 (0.5)	0.990 (0.010)
R-40	41.8 (1.7)	1874 (48)	22.9 (0.9)	26.2 (0.4)	0.169 (0.010)	4.9 (0.3)	0.047 (0.012)
R-41	43.7 (0.5)	1404 (110)	17.2 (1.4)	27.0 (0.3)	0.130 (0.006)	3.5 (0.1)	0.007 (0.006)
R-42	71.7 (3.3)	2217 (183)	18.1 (0.9)	22.7 (0.1)	0.189 (0.013)	5.7 (0.3)	0.100 (0.046)
R-43	28.5 (1.8)	2213 (55)	39.2 (0.5)	36.2 (1.2)	0.214 (0.006)	4.7 (0.2)	0.117 (0.015)
R-44	43.8 (2.6)	1870 (136)	27.5 (1.9)	30.1 (0.1)	0.163 (0.017)	3.9 (0.4)	0.040 (0.026)
R-45	87.0 (1.8)	3305 (75)	31.5 (0.4)	24.0 (0.3)	0.304 (0.008)	8.4 (0.3)	0.480 (0.035)
R-46	52.1 (0.8)	2831 (128)	28.4 (0.3)	27.8 (0.3)	0.257 (0.008)	7.0 (0.2)	0.297 (0.025)

**Appendix B. Supplementary data**

Supplementary material related to this article can be found, in the online version, at doi:<https://doi.org/10.1016/j.jsams.2019.10.006>.

**References**

- Cullen SJ, Donohoe A, McGoldrick A et al. Physiological and health characteristics of ex-jockeys. *J Sci Med Sport* 2016; 19(4):283–287.
- Huber BR, Alosco ML, Stein TD et al. Potential long-term consequences of concussive and subconcussive injury. *Phys Med Rehabil Clin* 2016; 27:503–511.
- O'Connor S, Warrington G, McGoldrick A et al. Race day concussion incidence in Irish professional flat and jump horse racing from 2011 to 2016. *J Sci Med Sport* 2017; 20(S3):20–21.
- Bond GR, Christoph RA, Rodgers BM. Pediatric equestrian injuries: assessing the impact of helmet use. *Pediatrics* 1995; 95:487–489.
- Petridou E, Kedikoglou S, Belechrli M et al. The mosaic of equestrian-related injuries in Greece. *J Trauma Acute Care Surg* 2004; 56:643–647.
- Smartt P, Chalmers D. A new look at horse-related sport and recreational injury in New Zealand. *J Sci Med Sport* 2009; 12(3):376–382.
- Forero Rueda MA, Halley WL, Gilchrist MD. Fall and injury incidence rates of jockeys while racing in Ireland, France and Britain. *Injury* 2010; 41:533–539.
- McCrorry P, Turner M, LeMasson B et al. An analysis of injuries resulting from professional horse racing in France during 1991–2001: a comparison with injuries

resulting from professional horse racing in Great Britain during 1992–2001. *Br J Sports Med* 2006; 40:614–618.

- ASTM F1163-15. Standard Specification for Protective Headgear Used in Horse Sports and Horseback Riding. In: *ASTM F1163-15*. American Society for Testing and Materials, 2015.
- EN 1384:2016. *Helmets for equestrian activities*, British Standards Institution: European CE Standards, 2016.
- PAS015:2011. *Helmets for equestrian use*, British Standards Institution, 2011.
- Mills N, Whitlock M. Performance of horse-riding helmets in frontal and side impacts. *Injury* 1989; 20:189–192.
- Pellman EJ, Viano DC, Tucker AM et al. Concussion in professional football: reconstruction of game impacts and injuries. *Neurosurgery* 2003; 53:799–814.
- McIntosh AS, Patton DA, Fréchède B et al. The biomechanics of concussion in unhelmeted football players in Australia: a case-control study. *BMJ Open* 2014; 4:e005078.
- Zhang L, Yang KH, King AI. A proposed injury threshold for mild traumatic brain injury. *J Biomech Eng* 2004; 126:226–236.
- Giordano C, Kleiven S. Evaluation of axonal strain as a predictor for mild traumatic brain injuries using finite element modeling. *Stapp Car Crash J* 2014; 58:29.
- Patton DA, McIntosh AS, Kleiven S. The biomechanical determinants of concussion: Finite element simulations to investigate tissue-level predictors of injury during sporting impacts to the unprotected head. *J Appl Biomech* 2015; 31:264–268.
- Oeur A, Gilchrist MD, Hoshizaki TB. Interaction of impact parameters for simulated falls in sport using three different sized Hybrid III headforms. *Int J Crashworthiness* 2019; 24(3):326–335.
- Forero Rueda MA, Gilchrist M. Racetrack turf impact measurements for jockey head injury risk analysis. *STARSS Conference*, 2007.

20. Bourdet N, Willinger R. Head impact conditions in case of equestrian accident, *IRCOBI Conference*, 2015, p. 156–167.
21. Post A, Koncan D, Kendall M et al. Analysis of speed accuracy using video analysis software. *Sports Eng* 2018; 21:235–241.
22. Doorly MC, Gilchrist MD. The use of accident reconstruction for the analysis of traumatic brain injury due to head impacts arising from falls. *Comput Methods Biomechan Biomed Eng* 2006; 9:371–377.
23. Clark JM, Connor TA, Post A et al. Could a compliant foam anvil characterise the biofidelic impact response of equestrian helmets? *J Biomech Eng* 2019. In Press.
24. Horgan TJ, Gilchrist MD. The creation of three-dimensional finite element models for simulating head impact biomechanics. *Int J Crashworthiness* 2003; 8:353–366.
25. Horgan TJ, Gilchrist MD. Influence of FE model variability in predicting brain motion and intracranial pressure changes in head impact simulations. *Int J Crashworthiness* 2004; 9:401–418.
26. Hutchison MG, Comper P, Meeuwisse WH et al. A systematic video analysis of National Hockey League (NHL) concussions, part II: how concussions occur in the NHL. *Br J Sports Med* 2015; 49:552–555.
27. Rowson S, Duma SM, Beckwith JG et al. Rotational head kinematics in football impacts: an injury risk function for concussion. *Anal Biomed Eng* 2012; 40:1–13.
28. Post A, Hoshizaki TB, Karton C et al. The biomechanics of concussion for ice hockey head impact events. *Comput Methods Biomech Biomed Eng* 2019; 22(6):631–643.
29. Kimpara H, Iwamoto M. Mild traumatic brain injury predictors based on angular accelerations during impacts. *Anal Biomed Eng* 2012; 40:114–126.
30. Bak K, Kalms S, Olesen S et al. Epidemiology of injuries in gymnastics. *Scand J Med Sci Sports* 1994; 4:148–154.